

A general frequency adaptive framework for damped response analysis of wind turbines

S. Adhikari^a, S. Bhattacharya^{b,*}

^aCollege of Engineering, Swansea University, Swansea, UK

^bDepartment of Civil and Environmental Engineering University of Surrey, Guildford, Surrey, UK

Abstract

Dynamic response analysis of wind turbine towers plays a pivotal role in their analysis, design, stability, performance and safety. Despite extensive research, the quantification of general dynamic response remains challenging due to an inherent lack of the ability to model and incorporate damping from a physical standpoint. This paper develops a frequency adaptive framework for the analysis of the dynamic response of wind turbines under general harmonic forcing with a damped and flexible foundation. The proposed method is founded on an augmented dynamic stiffness formulation based on an Euler-Bernoulli beam-column with elastic end supports along with tip mass and rotary inertia arising from the nacelle of the wind turbine. The dynamic stiffness coefficients are derived from the complex-valued transcendental displacement function which is the exact solution of the governing partial differential equation with appropriate boundary conditions. The closed-form analytical expressions of the dynamic response derived in the paper are exact and valid for higher frequency ranges. The proposed approach avoids the classical modal analysis and consequently the ad-hoc use of the modal damping factors are not necessary. It is shown that the damping in the wind turbine dynamic analysis is completely captured by seven different physically-realistic damping factors. Numerical results shown in the paper quantify the distinctive nature of the impact of the different damping factors. The exact closed-form analytical expressions derived in the paper can be used for benchmarking related experimental and finite element studies and at the initial design/analysis stage.

Keywords: Wind turbine; dynamic response; damping; foundation stiffness; harmonic excitation; offshore

1. Introduction

The United Nations has recently declared that we are facing a grave climate emergency and some of the most common manifestations are continuous ocean and atmospheric warming, heat waves and rise in sea level. A practical way to combat climate change

*Corresponding author. Tel: +44 (0)1483 689534

Email addresses: S.Adhikari@swansea.ac.uk (S. Adhikari), s.bhattacharya@surrey.ac.uk (S. Bhattacharya)

13 and to achieve net-zero emission target to run a country mostly on electricity produced
14 from renewable sources without burning much fossil fuel. Offshore wind turbines have the
15 proven potential for the island and coastal nations and as a result, there is a tremendous
16 rise in the proportion of electricity generation from such sources.

17 Offshore Wind Turbines are being currently constructed around the world and in
18 extremely challenging sites, see for example deeper water developments and using floating
19 system (Hywind in Scotland, see [1]), the typhoon and hurricane sites in Japan and China,
20 seismic locations in Taiwan, China, Korea and India [2]. These sites often apply dynamic
21 loading to the structure and the magnitude depends on the location. Due to its shape and
22 form, offshore wind turbine structures are dynamically sensitive as a large rotating mass is
23 applied at the top of the long slender column. Furthermore, the natural frequency of these
24 structures is also close to the forcing frequencies. The typical natural frequency of a 3.6
25 MW turbine is about 0.33Hz and that of an 8MW is 0.22Hz. As the turbines get larger,
26 the target natural frequency of the overall wind turbine system gets lower and comes near
27 to the wave frequencies. In some offshore development, predicting dynamic responses
28 becomes the main challenge. For example, the predominant wave period in Yellow sea
29 and Bohai sea (Chinese waters) is about 4.8 to 5 sec [3] and wave loading becomes a
30 critical design consideration for turbines above 8MW. There are other considerations
31 such as corrosion and fatigue [4] and scour [5]. The readers are referred to studies on
32 dynamics of offshore wind turbine by Zuo et al [6], Sellami et al [7], Banerjee et al [8] and
33 Sclavounos et al [9].

34 Guided by Limit State philosophy, a design must satisfy the following limit states:
35 ULS (Ultimate Limit State), SLS (Serviceability Limit State), FLS (Fatigue Limit State)
36 and ALS (Accidental Limit State). To evaluate any of the above limit states for different
37 dynamic load scenarios, the response of the structure must be evaluated. A quick method
38 of evaluation of dynamic helps to optimize the design of a given turbine (for a given
39 RNA mass and 1P frequency range) at a given site (wind field and wave/sea states)
40 through the change in physical parameters i.e. foundation stiffness and tower stiffness. In
41 certain challenging sites where the forcing frequency is very close to the natural frequency,
42 damping plays a beneficial role in optimization. There are different sources of damping
43 in an offshore wind turbine: Aerodynamic, hydrodynamic, structural damping, material
44 damping (including the soil). Recently several authors have considered explicit dynamic
45 analysis of wind turbine structures. Bending, axial and torsional vibrations of wind
46 turbines has been considered by Wang et al [10] and Vitor Chaves et al [11]. Due to
47 the interest of understanding the performance of offshore wind turbines in seismic areas,
48 dynamic analysis work is being conducted by He et al [12], Patra and Haldar [13], Zhao
49 M et al [14] and Jiang W et al [15]. These studies clearly demonstrate the need for
50 comprehensive dynamic analysis of wind turbine structures.

51 It has also been established that Soil-Structure Interaction (SSI) is very important
52 for predicting the short term and long-term performance of these structures. For design
53 purposes SSI can be classified as follows: (1) Load transfer mechanism from the founda-
54 tion to the soil (2) Modes of vibration of the whole system (3) Long term performance in
55 the sense whether or not the foundation will tilt progressively under the combined action
56 of millions of cycles of loads arising from the wind, wave and 1P (rotor frequency) and
57 2P/3P (blade passing frequency). In a series of previous studies, the authors [16–19] con-

58 sidered the analysis of the first natural frequency of wind turbines taking SSI into account.
59 The recent trend in wind turbine design is towards very large systems. While such large
60 systems give more power output, a potential disadvantage is that they can be susceptible
61 to dynamic loads as the natural frequencies become lower. As a result, many resonance
62 frequencies of the structure will be excited within the operating frequency ranges. There-
63 fore, for a credible dynamic analysis, it is necessary to have a simple approach which can
64 take account of multiple natural frequencies and vibration modes.

65 It is certainly possible to perform a classical modal analysis [20] for high-frequency
66 vibration problems. However, there are two major issues. Firstly, analytical solutions
67 for the natural frequencies and mode shapes are generally difficult to obtain beyond
68 the first mode. Secondly, simplified proportional modal damping assumptions must be
69 employed for the response analysis. One way these issues can be avoided is by using
70 the dynamic stiffness method [21–25]. This approach can be considered within the broad
71 class of spectral methods [26] for linear dynamical systems. A key feature of the dynamic
72 stiffness method is the use of complex shape functions (due to the presence of damping)
73 which are frequency-dependent [27]. The mass distribution of the element is treated
74 exactly in deriving the element dynamic stiffness matrix. The method does not employ
75 eigenfunction expansions and, consequently, a major step of the traditional finite element
76 analysis, namely, the determination of natural frequencies and mode shapes, is eliminated
77 which automatically avoids the errors due to series truncation [28]. Since the modal
78 expansion is not employed, ad hoc assumptions concerning the damping matrix being
79 proportional to the mass and/or stiffness are not necessary. The dynamic stiffness matrix
80 of one-dimensional structural elements, taking into account the effects of flexure, torsion,
81 axial and shear deformation, and damping, is exactly determinable, which, in turn, enables
82 the exact vibration analysis by an inversion of the global dynamic stiffness matrix [22].
83 The method is essentially a frequency-domain approach suitable for steady-state harmonic
84 or stationary random excitation problems. The static stiffness matrix and the consistent
85 mass matrix appear as the first two terms in the Taylor expansion [21, 29] of the dynamic
86 stiffness matrix in the frequency parameter.

87 The overview of the paper is as follows. In Section 2 an overview of dynamic stiffness
88 of undamped beam-columns is given. In particular, the equation of motion is discussed
89 in Subsection 2.1, the characteristic equation and essential non-dimensional parameters
90 are explained in Subsection 2.2 and the undamped dynamic stiffness matrix is derived
91 in Subsection 2.3. The dynamic stiffness matrix for damped beam-columns are derived
92 in Section 3. The effect of end restraints and tip mass is considered in Section 4. The
93 consideration of tip mass and rotary inertia is discussed in Subsection 4.1, while the con-
94 sideration of damped and flexible foundation is proposed in Subsection 4.2. The analysis
95 of dynamic response in the frequency domain is developed in Section 5 where exact closed-
96 form expressions have been derived for systems with fixed foundation (Subsection 5.1) and
97 systems with damped and flexible foundation (Subsection 5.2). The new expressions de-
98 rived in the paper is summarised in Section 6 and main conclusions are drawn in Section 7.

99 **2. Overview of dynamic stiffness of undamped beam-columns**

100 In Fig. 1, the schematic diagram of wind turbine tower constrained by flexible springs is
101 shown. An Euler-Bernoulli beam model is used to mathematically represent the dynamics

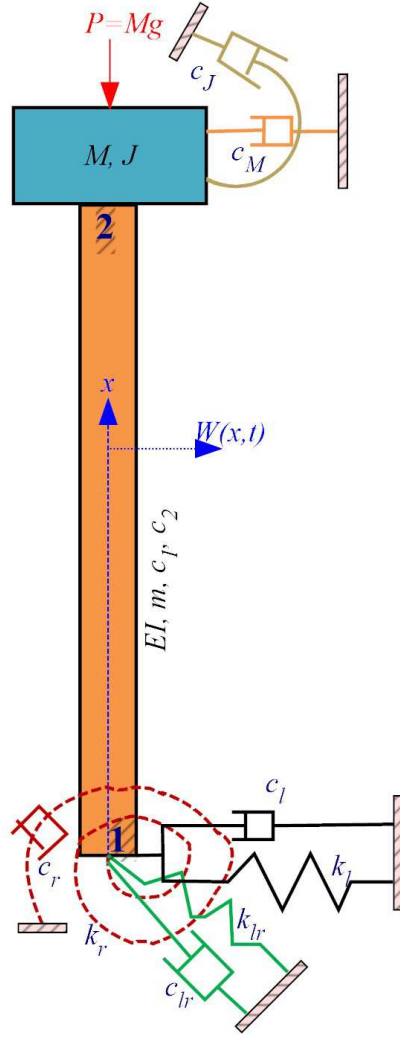


Fig. 1: A damped Euler Bernoulli beam with a top mass and point dampers are employed for dynamic analysis of a wind turbine tower. Dynamic foundation-structure interaction is modelled by three flexible springs and dampers. The mass of the blades and the rotor-hub are assumed to be M . The damping parameters c_M and c_J denote aerodynamic damping corresponding to linear and rotary motion of the top mass (nacelle). c_1 is the strain-rate-dependent viscous damping coefficient and c_2 is the velocity-dependent viscous damping coefficient of the wind turbine tower. c_r , c_l and c_{lr} correspond to rotational, lateral and coupling damping coefficients of the foundation.

102 of the beam. The bending stiffness of the beam is EI and the beam is attached to the
 103 foundation. Here x is the spatial coordinate, starting at the bottom and moving along the
 104 height of the structure. The interaction of the structure with the foundation is modelled
 105 using two springs. The rotational spring with spring stiffness k_r , the lateral spring with
 106 spring stiffness k_l and the coupling spring with spring stiffness k_{lr} constrains the system
 107 at the bottom ($x = 0$). The beam has a top mass with rotary inertia J and mass M .
 108 This top mass is used to idealise the rotor and blade system. The mass per unit length of
 109 the beam is m and the beam is subjected to a constant compressive axial load $P = Mg$.
 110 Although the motivation of this study is arising from the large offshore wind turbines,
 111 the analytical formulation proposed here is not restricted to offshore wind turbines. With

112 suitable values of k_r , k_l and k_{lr} , this analysis can be applied on onshore wind turbines
 113 also.

114 2.1. Equation of motion

115 The fourth-order partial differential equation describing the equation of motion of an
 116 Euler Bernoulli beam (see for example [20, 30, 31]) is given by

$$EI \frac{\partial^4 W(x, t)}{\partial x^4} + P \frac{\partial^2 W(x, t)}{\partial x^2} + m \ddot{W}(x, t) = F(x, t) \quad (1)$$

117 Here $W(x, t)$ is the transverse deflection of the beam, t is time, $\dot{(\bullet)}$ denotes derivative with
 118 respect to time and $F(x, t)$ is the applied time depended load on the beam. The height
 119 of the structure is considered to be L . Our central aim is to obtain the dynamic resposne
 120 in the frequency domain *without* calculating the natural frequencies of the system. Here
 121 we develop an approach based on the non-dimensionalisation of the equation of motion
 122 (1) in conjunction with the dynamic stiffness method.

123 2.2. Characteristic equation and non-dimensional parameters

124 In previous works [16–19] the authors developed a method for the calculation of the
 125 natural frequencies of system (1) based on the non-dimensionalisation of the equation of
 126 motion and the boundary conditions. A complete different strategy is adopted here. The
 127 aim is to express the dynamics of the beam by a finite-element like discretised system.
 128 However, unlike the conventional finite element method where frequency-independent
 129 cubic polynomial is used for discretisation, we aim to use functions which ere the exact
 130 solutions of the dynamic system. This functions arise from the characteristic equation as
 131 discussed below.

132 We consider free vibration so that the forcing can be assumed to be zero. Assuming
 133 harmonic solution we have

$$W(x, t) = w(\xi) \exp \{i\omega t\} \quad (2)$$

134 where $i = \sqrt{-1}$, ω is the excitation frequency and the normalised length

$$\xi = x/L \quad (3)$$

Substituting this in the equation of motion one has

$$\frac{EI}{L^4} \frac{d^4 w(\xi)}{d\xi^4} + \frac{P}{L^2} \frac{d^2 w(\xi)}{d\xi^2} - m\omega^2 w(\xi) = 0 \quad (4)$$

$$\text{or } \frac{d^4 w(\xi)}{d\xi^4} + \nu \frac{d^2 w(\xi)}{d\xi^2} - \Omega^2 w(\xi) = 0 \quad (5)$$

135 Here the non-dimensional parameters can be identified as

$$\nu = \frac{PL^2}{EI} \quad (\text{nondimensional axial force})$$

$$\Omega^2 = \omega^2 \frac{mL^4}{EI} = \omega^2 c^2 \quad (\text{nondimensional frequency parameter}) \quad (6)$$

$$\text{where } c^2 = \frac{mL^4}{EI} \quad (\text{frequency scaling parameter})$$

136 The effect of rotary inertia is ignored in the above formulation. If this effect is to be
 137 included, then ν should be replaced by [16, 18] by $\tilde{\nu}$ defined as

$$\tilde{\nu} = \nu + \mu^2 \Omega^2 \quad (7)$$

138 where

$$\mu = \frac{r}{L} \quad (\text{nondimensional radius of gyration}) \quad (8)$$

139 Assuming a solution of the form

$$w(\xi) = \exp \{ \lambda \xi \} \quad (9)$$

140 and substituting in the equation of motion (4) results

$$\lambda^4 + \nu \lambda^2 - \Omega^2 = 0 \quad (10)$$

141 This equation is often known as the dispersion relationship. This is the equation which
 142 underpins the dynamic shape functions of the beam. Solving this equation for λ^2 we have

$$\begin{aligned} \lambda^2 &= -\frac{\nu}{2} \pm \sqrt{\left(\frac{\nu}{2}\right)^2 + \Omega^2} \\ &= -\left(\underbrace{\sqrt{\left(\frac{\nu}{2}\right)^2 + \Omega^2} + \frac{\nu}{2}}_{\lambda_1^2}\right), \quad \left(\underbrace{\sqrt{\left(\frac{\nu}{2}\right)^2 + \Omega^2} - \frac{\nu}{2}}_{\lambda_2^2}\right) \end{aligned} \quad (11)$$

143 Because ν^2 and Ω^2 are always positive quantities, both roots are real with one negative
 144 and one positive root. Therefore, the four roots can be expressed as

$$\lambda = \pm i \lambda_1, \quad \pm \lambda_2 \quad (12)$$

where

$$\lambda_1 = \left(\sqrt{\left(\frac{\nu}{2}\right)^2 + \Omega^2} + \frac{\nu}{2} \right)^{1/2} \geq 0 \quad (13)$$

$$\text{and } \lambda_2 = \left(\sqrt{\left(\frac{\nu}{2}\right)^2 + \Omega^2} - \frac{\nu}{2} \right)^{1/2} \geq 0 \quad (14)$$

145 In view of the roots in equation (12), the solution $w(\xi)$ can be expressed as

$$\begin{aligned} w(\xi) &= w_1 \sin \lambda_1 \xi + w_2 \cos \lambda_1 \xi + w_3 \sinh \lambda_2 \xi + w_4 \cosh \lambda_2 \xi \\ \text{or } w(\xi) &= \mathbf{s}^T(\xi) \mathbf{w} \end{aligned} \quad (15)$$

where the vectors

$$\mathbf{s}(\xi, \omega) = \{ \cos \lambda_1 \xi, \sin \lambda_1 \xi, \cosh \lambda_2 \xi, \sinh \lambda_2 \xi \}^T \quad (16)$$

$$\text{and } \mathbf{w} = \{ w_1, w_2, w_3, w_4 \}^T \quad (17)$$

146 Next we use these solutions to obtain the dynamic shape functions of the beam.

147 *2.3. Undamped dynamic stiffness matrix*

148 *2.3.1. Frequency dependent shape functions*

149 For classical (static) finite element analysis of beams, cubic polynomials are used as
 150 shape functions (see for example [32]). Here we aim to incorporate frequency depen-
 151 dent dynamic shape functions, as used with the framework of the dynamic finite element
 152 method. The dynamic shape functions are obtained such that the equation of dynamic
 153 equilibrium is satisfied exactly at all points within the element. Similar to the classi-
 154 cal finite element method, assume that the frequency-dependent displacement within an
 155 element is interpolated from the nodal displacements as

$$w(\xi, \omega) = \mathbf{N}^T(\xi, \omega) \mathbf{w}(\omega) \quad (18)$$

156 Here $\mathbf{w}(\omega) \in \mathbb{R}^n$ is the nodal displacement vector $\mathbf{N}(\xi, \omega) \in \mathbb{R}^n$ is the vector of frequency-
 157 dependent shape functions and $n = 4$ is the number of the nodal degrees-of-freedom.
 158 Using the vector of the basis functions $\mathbf{s}(\xi, \omega)$ in Eq. (16), the shape function vector can
 159 be expressed as

$$\mathbf{N}^T(\xi, \omega) = \mathbf{s}^T(\xi, \omega) \mathbf{\Gamma}(\omega) \quad (19)$$

160 The matrix $\mathbf{\Gamma}(\omega) \in \mathbb{C}^{4 \times 4}$ depends on the boundary conditions. An element for the damped
 beam under bending vibration is shown in Fig. 2.

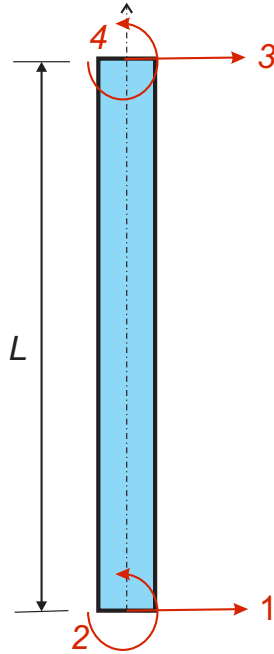


Fig. 2: A dynamic element for the bending vibration of a beam. It has two nodes and four degrees of freedom. The displacement field within the element is expressed by frequency dependent shape functions.

161 The relationship between the shape functions and the boundary conditions can be
 162 represented as in Table 1, where boundary conditions in each column give rise to the
 163 corresponding shape function. Writing Eq. (18) for the above four sets of boundary
 164 conditions, one obtains
 165

$$[\mathbf{R}] \left[\widehat{\mathbf{w}}^{(1)}, \widehat{\mathbf{w}}^{(2)}, \widehat{\mathbf{w}}^{(3)}, \widehat{\mathbf{w}}^{(4)} \right] = \mathbf{I} \quad (20)$$

Table 1: The four different boundary conditions used to derive the dynamic shape functions of the beam.

	$N_1(\xi, \omega)$	$N_2(\xi, \omega)$	$N_3(\xi, \omega)$	$N_4(\xi, \omega)$
$w(0, \omega)$	1	0	0	0
$\left. \frac{dw(\xi, \omega)}{d\xi} \right _{\xi=0}$	0	1	0	0
$w(1, \omega)$	0	0	1	0
$\left. \frac{dw(\xi, \omega)}{d\xi} \right _{\xi=1}$	0	0	0	1

166 where (omitting ω for convenience)

$$\mathbf{R} = \begin{bmatrix} s_1(0) & s_2(0) & s_3(0) & s_4(0) \\ \frac{ds_1}{d\xi}(0) & \frac{ds_2}{d\xi}(0) & \frac{ds_3}{d\xi}(0) & \frac{ds_4}{d\xi}(0) \\ s_1(1) & s_2(1) & s_3(1) & s_4(1) \\ \frac{ds_1}{d\xi}(1) & \frac{ds_2}{d\xi}(1) & \frac{ds_3}{d\xi}(1) & \frac{ds_4}{d\xi}(1) \end{bmatrix} = \begin{bmatrix} 1 & 0 & 1 & 0 \\ 0 & \lambda_1 & 0 & \lambda_2 \\ \cos(\lambda_1) & \sin(\lambda_1) & \cosh(\lambda_2) & \sinh(\lambda_2) \\ -\sin(\lambda_1)\lambda_1 & \cos(\lambda_1)\lambda_1 & \sinh(\lambda_2)\lambda_2 & \cosh(\lambda_2)\lambda_2 \end{bmatrix} \quad (21)$$

167 and $\widehat{\mathbf{w}}^{(k)}$ is the vector of constants giving rise to the k -th shape function. In view of the
168 boundary conditions represented in Table 1 and equation (20), the shape functions for
169 bending vibration can be shown to be given by Eq. (19) where

$$\mathbf{\Gamma}(\omega) = \left[\widehat{\mathbf{w}}^{(1)}, \widehat{\mathbf{w}}^{(2)}, \widehat{\mathbf{w}}^{(3)}, \widehat{\mathbf{w}}^{(4)} \right] = [\mathbf{R}^{-1}] = \frac{1}{\lambda_1^2 + \lambda_2^2} \begin{bmatrix} \lambda_2^2 - \Gamma_4 & \Gamma_2 L & -\Gamma_3 & \Gamma_1 L \\ -\frac{\Gamma_6}{\lambda_1} & \left(\lambda_1 + \frac{\Gamma_4}{\lambda_1} \right) L^{-1} & -\frac{\Gamma_5}{\lambda_1} & -\frac{\Gamma_3 L}{\lambda_1} \\ \lambda_1^2 + \Gamma_4 & -F_2 L & \Gamma_3 & -\Gamma_1 L \\ \frac{\Gamma_6}{\lambda_2} & \left(\lambda_2 - \frac{\Gamma_4}{\lambda_2} \right) L^{-1} & \frac{\Gamma_5}{\lambda_2} & \frac{\Gamma_3 L}{\lambda_2} \end{bmatrix} \quad (22)$$

170 Following [22] the functions $\Gamma_j, j = 1, 2, \dots, 6$ can be defined as

$$\begin{aligned} \Gamma_1 &= (\lambda_2 \sin(\lambda_1) - \lambda_1 \sinh(\lambda_2)) (\lambda_1^2 + \lambda_2^2) / \Delta \\ \Gamma_2 &= (\lambda_1 \cos(\lambda_1) \sinh(\lambda_2) - \lambda_2 \sin(\lambda_1) \cosh(\lambda_2)) (\lambda_1^2 + \lambda_2^2) / \Delta \\ \Gamma_3 &= (\cos(\lambda_1) - \cosh(\lambda_2)) \lambda_1 \lambda_2 (\lambda_1^2 + \lambda_2^2) / \Delta \\ \Gamma_4 &= ((\lambda_1^2 - \lambda_2^2) (1 - \cos(\lambda_1) \cosh(\lambda_2)) + 2 \lambda_1 \lambda_2 \sin(\lambda_1) \sinh(\lambda_2)) \lambda_1 \lambda_2 / \Delta \\ \Gamma_5 &= (\lambda_2 \sinh(\lambda_2) + \lambda_1 \sin(\lambda_1)) \lambda_1 \lambda_2 (\lambda_1^2 + \lambda_2^2) / \Delta \\ \Gamma_6 &= -(\lambda_1 \cosh(\lambda_2) \sin(\lambda_1) + \lambda_2 \sinh(\lambda_2) \cos(\lambda_1)) \lambda_1 \lambda_2 (\lambda_1^2 + \lambda_2^2) / \Delta \end{aligned} \quad (23)$$

171 Here Δ , related to the determinant of the matrix \mathbf{R} , is given by

$$\Delta = -\det(\mathbf{R}) = 2 \lambda_1 \lambda_2 (\cos(\lambda_1) \cosh(\lambda_2) - 1) + (\lambda_1^2 - \lambda_2^2) \sin(\lambda_1) \sinh(\lambda_2) \quad (24)$$

172 The above equations completely defines the shape function. Next we use them to obtain
173 the dynamic stiffness matrix.

174 2.3.2. Element dynamic stiffness matrix and the forcing vector

175 The stiffness and mass matrices can be obtained following the conventional variational
176 formulation [33]. The only difference is instead of classical cubic polynomials as the shape

177 functions, frequency dependent shape functions in (19) should be used. The dynamic
178 stiffness matrix is defined as

$$\mathbf{D}(\omega) = \mathbf{K}(\omega) - \mathbf{G}(\omega) - \omega^2 \mathbf{M}(\omega) \quad (25)$$

179 so that the equation of dynamic equilibrium of the element is given be

$$\mathbf{D}(\omega) \mathbf{w}(\omega) = \mathbf{f}(\omega) \quad (26)$$

180 Here $\mathbf{f}(\omega)$ element forcing vector and the response vector $\mathbf{w}(\omega)$ is given by

$$\mathbf{w}(\omega) = \begin{Bmatrix} w_1(\omega) \\ w_2(\omega) \\ w_3(\omega) \\ w_4(\omega) \end{Bmatrix} = \begin{Bmatrix} \delta^{(1)}(\omega) \\ \theta^{(1)}(\omega) \\ \delta^{(2)}(\omega) \\ \theta^{(2)}(\omega) \end{Bmatrix} \quad (27)$$

Here $\delta^{(1)}(\omega)$, $\theta^{(1)}(\omega)$ and $\delta^{(2)}(\omega)$, $\theta^{(2)}(\omega)$ denotes the frequency dependent displacement and rotation at the bottom and top end of the wind-turbine tower respectively. In Eq. (25), the frequency-dependent stiffness, geometric stiffness and mass matrices can be obtained from

$$\mathbf{K}(\omega) = EI \int_0^L \frac{d^2 \mathbf{N}(x/L, \omega)}{dx^2} \frac{d^2 \mathbf{N}^T(x/L, \omega)}{dx^2} dx = \frac{EI}{L^3} \int_0^1 \frac{d^2 \mathbf{N}(\xi, \omega)}{d\xi^2} \frac{d^2 \mathbf{N}^T(\xi, \omega)}{d\xi^2} d\xi \quad (28)$$

$$\mathbf{G}(\omega) = P \int_0^L \frac{d\mathbf{N}(x/L, \omega)}{dx} \frac{d\mathbf{N}^T(x/L, \omega)}{dx} dx = PL \int_0^1 \frac{d\mathbf{N}(\xi, \omega)}{d\xi} \frac{d\mathbf{N}^T(\xi, \omega)}{d\xi} d\xi \quad (29)$$

$$\text{and } \mathbf{M}(\omega) = m \int_0^L \mathbf{N}(x/L, \omega) \mathbf{N}^T(x/L, \omega) dx = mL \int_0^1 \mathbf{N}(\xi, \omega) \mathbf{N}^T(\xi, \omega) d\xi \quad (30)$$

181 After some algebraic simplifications, it can be shown [22] that the dynamic stiffness matrix
182 is given by the following closed-form expression

$$\mathbf{D}(\omega) = \frac{EI}{L^3} \begin{bmatrix} \Gamma_6 & -\Gamma_4 L & \Gamma_5 & \Gamma_3 L \\ -\Gamma_4 L & \Gamma_2 L^2 & -\Gamma_3 L & \Gamma_1 L^2 \\ \Gamma_5 & -\Gamma_3 L & \Gamma_6 & \Gamma_4 L \\ \Gamma_3 L & \Gamma_1 L^2 & \Gamma_4 L & \Gamma_2 L^2 \end{bmatrix} \quad (31)$$

183 The functions $\Gamma_j, j = 1, 2, \dots, 6$ are defined in (23). The elements of this matrix are
184 frequency dependent quantities because λ_1 and λ_2 are functions of ω .

185 Considering the frequency representation of the forcing function in Eq. (1) we have

$$F(x, t) = f(\xi, \omega) \exp\{i\omega t\} \quad (32)$$

186 where $f(\xi, \omega)$ is in general a spatially varying frequency dependent forcing function. Using
187 this, the element forcing vector is defined as

$$\mathbf{f}(\omega) = \int_0^L f(x/L, \omega) \mathbf{N}(x/L, \omega) dx = L \mathbf{\Gamma}^T(\omega) \int_0^1 f(\xi, \omega) \mathbf{s}(\xi, \omega) d\xi \quad (33)$$

188 For a perfect harmonic excitation $f(\xi, \omega)$ is constant with respect the frequency. In
189 addition, if the forcing is uniformly distributed over the length, then $f(\xi, \omega)$ is constant
190 with respect to the non-dimension length parameter ξ also.

191 As dynamic stiffness is based on the exact solution of the governing differential equa-
192 tion, only one element is necessary to represent the entire beam for all frequency values.

193 Therefore the 4 matrix equation in (26) described the exact dynamic of the wind turbine
 194 tower for any excitation frequency. So far damping in the system has not been considered.
 195 Without the consideration of damping, Eq. (26) becomes singular for certain frequencies
 196 and therefore cannot be numerically used for all frequency values. In the next section we
 197 include damping effects in the equation of motion.

198 3. Dynamic stiffness of damped beam-columns

199 3.1. Systems with general damping

200 The equation of motion of a damped beam-column can be expressed as

$$EI \frac{\partial^4 W(x, t)}{\partial x^4} + c_1 \frac{\partial^5 W(x, t)}{\partial x^4 \partial t} + P \frac{\partial^2 W(x, t)}{\partial x^2} + c_2 \frac{\partial W(x, t)}{\partial t} + m \ddot{W}(x, t) = F(x, t) \quad (34)$$

It is assumed that the behaviour of the beam follows the Euler-Bernoulli hypotheses as before. In the above equation c_1 is the strain-rate-dependent viscous damping coefficient and c_2 is the velocity-dependent viscous damping coefficient. Considering harmonic motion with frequency ω as in Eq. (2) we have

$$\frac{EI}{L^4} \frac{d^4 w(\xi)}{d\xi^4} + i\omega \frac{c_1}{L^4} \frac{d^4 w(\xi)}{d\xi^4} + \frac{P}{L^2} \frac{d^2 w(\xi)}{d\xi^2} + i\omega c_2 w(\xi) - m\omega^2 w(\xi) = 0 \quad (35)$$

$$\text{or} \quad \left(1 + i\omega \frac{c_1}{EI}\right) \frac{d^4 w(\xi)}{d\xi^4} + \nu \frac{d^2 w(\xi)}{d\xi^2} - \Omega^2 \left(1 - i \frac{c_2}{m\omega}\right) w(\xi) = 0 \quad (36)$$

201 Following the damping convention in dynamic analysis as in [20], we consider stiffness
 202 and mass proportional damping. Therefore, we express the damping constants as

$$\frac{c_1}{EI} = \xi_1 \sqrt{\frac{mL^4}{EI}} \quad \text{and} \quad \frac{c_2}{m} = \xi_2 / \sqrt{\frac{mL^4}{EI}} \quad (37)$$

where ξ_1 and ξ_2 are non-dimensional stiffness and mass proportional damping factors. From the above expressions, these non-dimensional constants can be explicitly expressed in terms of the damping coefficients as

$$\xi_1 = \frac{c_1}{L^2 \sqrt{m EI}} \quad (\text{strain-rate-dependent damping factor}) \quad (38)$$

$$\xi_2 = \frac{c_2 L^2}{\sqrt{m EI}} \quad (\text{velocity-dependent damping factor}) \quad (39)$$

203 Substituting these, Eq. (36) can be simplified as

$$(1 + i\Omega \xi_1) \frac{d^4 w(\xi)}{d\xi^4} + \nu \frac{d^2 w(\xi)}{d\xi^2} - \Omega^2 (1 - i\xi_2/\Omega) w(\xi) = 0 \quad (40)$$

The characteristic equation therefore can be obtained as

$$(1 + i\Omega \xi_1) \lambda^4 + \nu \lambda^2 - \Omega^2 (1 - i\xi_2/\Omega) = 0 \quad (41)$$

$$\text{or} \quad \lambda^4 + \nu_d \lambda^2 - \Omega_d^2 = 0 \quad (42)$$

where

$$\nu_d = \frac{\nu}{1 + i\Omega\xi_1} \quad (43)$$

$$\text{and } \Omega_d^2 = \Omega^2 \frac{(1 - i\xi_2/\Omega)}{(1 + i\Omega\xi_1)} \quad (44)$$

204 The dynamic stiffness matrix of the damped beam column can be obtained from the for-
205 mulation derived in the previous section by replacing ν and Ω with ν_d and Ω_d respectively.

206 3.2. Special cases

207 We consider some familiar special cases to relate the general result in the previous
208 section with known results.

209 3.2.1. Standard undamped beam without the axial force

210 For this case $\nu = 0$ and from equations (13) and (14) one obtains $\lambda_1 = \lambda_2 = \sqrt{\Omega} =$
211 $\sqrt{\omega} \sqrt{\frac{mL^4}{EI}} = \bar{\lambda}$ (say). Substituting these in equation (31) and simplifying we obtain the
212 dynamic stiffness matrix as

$$\mathbf{D}(\omega) = \frac{EI}{L^3} \begin{bmatrix} G_6 & -G_4L & G_5 & G_3L \\ -G_4L & G_2L^2 & -G_3L & G_1L^2 \\ G_5 & -G_3L & G_6 & G_4L \\ G_3L & G_1L^2 & G_4L & G_2L^2 \end{bmatrix} \quad (45)$$

213 where

$$\begin{aligned} G_1 &= \frac{\bar{\lambda} \sin(\bar{\lambda}) - \bar{\lambda} \sinh(\bar{\lambda})}{\cos(\bar{\lambda}) \cosh(\bar{\lambda}) - 1}, & G_2 &= \frac{\bar{\lambda} \sinh(\bar{\lambda}) \cos(\bar{\lambda}) - \bar{\lambda} \cosh(\bar{\lambda}) \sin(\bar{\lambda})}{\cos(\bar{\lambda}) \cosh(\bar{\lambda}) - 1} \\ G_3 &= \frac{(\cos(\bar{\lambda}) - \cosh(\bar{\lambda})) \bar{\lambda}^2}{\cos(\bar{\lambda}) \cosh(\bar{\lambda}) - 1}, & G_4 &= \frac{\bar{\lambda}^2 \sin(\bar{\lambda}) \sinh(\bar{\lambda})}{\cos(\bar{\lambda}) \cosh(\bar{\lambda}) - 1} \\ G_5 &= \frac{(\bar{\lambda} \sinh(\bar{\lambda}) + \bar{\lambda} \sin(\bar{\lambda})) \bar{\lambda}^2}{\cos(\bar{\lambda}) \cosh(\bar{\lambda}) - 1}, & G_6 &= -\frac{(\bar{\lambda} \cosh(\bar{\lambda}) \sin(\bar{\lambda}) + \bar{\lambda} \sinh(\bar{\lambda}) \cos(\bar{\lambda})) \bar{\lambda}^2}{\cos(\bar{\lambda}) \cosh(\bar{\lambda}) - 1} \end{aligned} \quad (46)$$

214 The dynamic stiffness matrix in (45) matches exactly with the dynamic stiffness matrix
215 of the Euler-Bernoulli beams as given in [21].

216 3.2.2. The static limit

217 When no axial force is present, the static limit is obtained by taking the mathematical
218 limit of $\omega \rightarrow 0$. Using this limit in the expression of $G_j, j = 1, \dots, 6$ in equations (46),
219 from the expression of the dynamic stiffness matrix in (45) we have

$$\mathbf{K}_{EB} = \lim_{\omega \rightarrow 0} \mathbf{D}(\omega) = \frac{EI}{L^3} \begin{bmatrix} 12 & 6L & -12 & 6L \\ 6L & 4L^2 & -6L & 2L^2 \\ -12 & -6L & 12 & -6L \\ 6L & 2L^2 & -6L & 4L^2 \end{bmatrix} \quad (47)$$

220 This limiting matrix is exactly the same as the conventional stiffness matrix for Euler-
221 Bernoulli beams [33]. Therefore, the dynamic stiffness matrix proposed here is a general-
222 isation in the frequency domain.

223 **4. Effect of end restraints and tip mass**

224 *4.1. The consideration of the top mass and rotary inertia*

225 The mass of the nacelle and rotor blades are represented by M in Fig. 1. This is very
 226 significant and can be more than the mass of the tower. Due to non-negligible geometric
 227 dimension, this mass cannot be modelled as a classical point mass. Therefore, rotary
 228 inertia of this mass should also be taken into account. We assume that the rotary inertia
 229 of the top mass is given by J . From practical experiences it is known that the top mass
 230 is subjected to significant aerodynamic damping. Therefore, this must also be taken into
 231 account in an exact and effective manner. In order to incorporate the effect of M and
 232 J , together with their corresponding damping within the scope of the dynamic stiffness
 233 approach, we consider a zero-length damped ‘finite element’ corresponding to the degree
 234 of freedom of the top point (point 2 in Fig. 1). The dynamic equilibrium of this element
 235 can be expressed by the following matrix equation

$$\underbrace{\begin{bmatrix} -\omega^2 M + i\omega c_M & 0 \\ 0 & -\omega^2 J + i\omega c_J \end{bmatrix}}_{\mathbf{D}_2(\omega)} \begin{Bmatrix} w_3 \\ w_4 \end{Bmatrix} = \begin{Bmatrix} f_3 \\ f_4 \end{Bmatrix} \quad (48)$$

Here the damping constants c_M and c_J correspond to linear and rotational damping of the top mass. Following the notations of the degrees of freedom in Fig. 2, it should be noted that w_3 is the displacement and w_4 is the rotation of the top point. We introduce the two following non-dimensional parameters

$$\alpha = \frac{M}{mL} \quad (\text{non-dimensional mass ratio}) \quad (49)$$

$$\beta = \frac{J}{mL^3} \quad (\text{non-dimensional rotary inertia}) \quad (50)$$

Using these quantities it can be deduced that

$$\omega^2 M = \omega^2 \alpha mL = \Omega^2 \frac{EI}{mL^4} \alpha mL = \frac{EI}{L^3} \Omega^2 \alpha \quad (51)$$

$$\omega^2 J = \omega^2 \beta mL^3 = \Omega^2 \frac{EI}{mL^4} \beta mL^3 = \frac{EI}{L^3} \Omega^2 \beta L^2 \quad (52)$$

236 As a result the dynamic stiffness matrix corresponding to the top mass element becomes

$$\mathbf{D}_2(\omega) = \frac{EI}{L^3} \begin{bmatrix} -\Omega^2 \bar{\alpha} & 0 \\ 0 & -\Omega^2 \bar{\beta} L^2 \end{bmatrix} \quad (53)$$

In the above equation, the complex frequency-dependent quantities $\bar{\alpha}$ and $\bar{\beta}$ are defined as

$$\bar{\alpha} = \alpha - i \frac{\xi_M}{\Omega} \quad (\text{damped non-dimensional mass ratio}) \quad (54)$$

$$\text{and } \bar{\beta} = \beta - i \frac{\xi_J}{\Omega} \quad (\text{damped non-dimensional rotary inertia}) \quad (55)$$

After some algebraic simplifications, the following new non-dimensional damping parameters are identified as

$$\xi_M = \frac{c_M L}{\sqrt{m EI}} \quad (\text{mass damping factor}) \quad (56)$$

$$\text{and } \xi_J = \frac{c_J}{L\sqrt{m EI}} \quad (\text{rotary damping factor}) \quad (57)$$

237 Adding this with the dynamic stiffness matrix of the beam we have the effective
238 stiffness matrix as

$$\mathbf{D}_e(\omega) = \frac{EI}{L^3} \begin{bmatrix} \Gamma_6 & -\Gamma_4 L & \Gamma_5 & \Gamma_3 L \\ -\Gamma_4 L & \Gamma_2 L^2 & -\Gamma_3 L & \Gamma_1 L^2 \\ \Gamma_5 & -\Gamma_3 L & (\Gamma_6 - \Omega^2 \bar{\alpha}) & \Gamma_4 L \\ \Gamma_3 L & \Gamma_1 L^2 & \Gamma_4 L & (\Gamma_2 - \Omega^2 \beta) L^2 \end{bmatrix} \quad (58)$$

239 Note that in the above summation, elements of $\mathbf{D}_2(\omega)$ are added with the elements of the
240 matrix $\mathbf{D}(\omega)$ corresponding to the relevant degrees of freedom (3 and 4 in this case).

241 4.2. The consideration of damped and flexible foundation

242 The importance of flexibility of foundation is now well recognised [34]. In the previous
243 works by the authors [16, 18] it was observed that the first undamped natural frequency of
244 the system is sensitive to the stiffness parameters related to the foundation. The effect of
245 damping in the foundation has never been taken into account in the context of dynamics of
246 wind turbine towers. Here we propose a novel and a simple approach to include the effect
247 of foundation stiffness and damping simultaneously by using the idea of a ‘zero-length
248 finite element’ corresponding to point 1 in Fig. 1. Three types of stiffness constants [19]
249 and three types of damping constants are used to model damped soil-structure interaction:

250 (a) Lateral spring and damper k_l and c_l

251 (b) Rotational spring and damper k_r and c_r

252 (c) Cross spring and damper k_{lr} and c_{lr}

253 The dynamic equilibrium for the virtual element corresponding to point 1 in Fig. 1 we
254 have the matrix equation

$$\underbrace{\begin{bmatrix} k_l + i\omega c_l & -(k_{lr} + i\omega c_{lr}) \\ -(k_{lr} + i\omega c_{lr}) & k_r + i\omega c_r \end{bmatrix}}_{\mathbf{D}_1(\omega)} \begin{Bmatrix} w_1 \\ w_2 \end{Bmatrix} = \begin{Bmatrix} 0 \\ 0 \end{Bmatrix} \quad (59)$$

255 Following the notations of the degrees of freedom in Fig. 2, it should be noted that w_1
256 is the displacement and w_2 is the rotation of the bottom point. The forcing vector is
257 considered to be zero as it is assumed that no net external forcing is applied at point 1.

We introduce the following non-dimensional stiffness parameters

$$\eta_l = \frac{k_l L^3}{EI} \quad (\text{nondimensional lateral foundation stiffness}) \quad (60)$$

$$\eta_r = \frac{k_r L}{EI} \quad (\text{nondimensional rotational foundation stiffness}) \quad (61)$$

$$\eta_{rl} = \frac{k_{rl} L^2}{EI} \quad (\text{nondimensional cross foundation stiffness}) \quad (62)$$

Using these, the following new non-dimensional damping parameters are introduced

$$\xi_l = \frac{c_l L}{\eta_l \sqrt{m EI}} \quad (\text{lateral foundation damping factor}) \quad (63)$$

$$\xi_r = \frac{c_r}{\eta_r L \sqrt{m EI}} \quad (\text{rotational foundation damping factor}) \quad (64)$$

$$\xi_{rl} = \frac{c_{rl}}{\eta_{rl} \sqrt{m EI}} \quad (\text{cross foundation damping factor}) \quad (65)$$

258 In view of these quantities, after some simplifications it can be shown that the dynamic
259 stiffness matrix corresponding to the damped foundation element becomes

$$\mathbf{D}_1(\omega) = \frac{EI}{L^3} \begin{bmatrix} \eta_l(1 + i\Omega\xi_l) & -\eta_{rl}(1 + i\Omega\xi_{rl})L \\ -\eta_{rl}(1 + i\Omega\xi_{rl})L & \eta_r(1 + i\Omega\xi_r)L^2 \end{bmatrix} \quad (66)$$

260 Adding this with the dynamic stiffness matrix of the beam we have the combined stiffness
261 matrix as

$$\mathbf{D}_e(\omega) = \frac{EI}{L^3} \begin{bmatrix} \bar{\Gamma}_6 & -\bar{\Gamma}_4 L & \Gamma_5 & \Gamma_3 L \\ -\bar{\Gamma}_4 L & \bar{\Gamma}_2 L^2 & -\Gamma_3 L & \Gamma_1 L^2 \\ \Gamma_5 & -\Gamma_3 L & (\Gamma_6 - \Omega^2 \bar{\alpha}) & \Gamma_4 L \\ \Gamma_3 L & \Gamma_1 L^2 & \Gamma_4 L & (\Gamma_2 - \Omega^2 \bar{\beta}) L^2 \end{bmatrix} \quad (67)$$

Note that in the above summation, elements of $\mathbf{D}_1(\omega)$ are added with the elements of the matrix $\mathbf{D}_e(\omega)$ corresponding to the relevant degrees of freedom (3 and 4 in this case). Therefore, in the above matrix

$$\bar{\Gamma}_6 = \Gamma_6 + \eta_l(1 + i\Omega\xi_l) \quad (68)$$

$$\bar{\Gamma}_4 = \Gamma_4 + \eta_{rl}(1 + i\Omega\xi_{rl}) \quad (69)$$

$$\text{and } \bar{\Gamma}_2 = \Gamma_2 + \eta_r(1 + i\Omega\xi_r) \quad (70)$$

262 Equation (67) represents the complete exact and the most general dynamic stiffness matrix
263 corresponding to the damped wind turbine tower model in Fig. 1. The elements of this
264 matrix is given by transcendental function of complex arguments. All the constants
265 necessary to obtain this matrix have been expressed in closed-form using non-dimensional
266 quantities. Next we develop the process of obtaining dynamic response due to selected
267 forcing functions.

268 **5. Dynamic response in the frequency domain**

269 *5.1. System with fixed foundation*

270 For systems with a fixed foundation the dynamic stiffness matrix in (58) is used. The
271 complete equilibrium equation is therefore given by

$$\frac{EI}{L^3} \begin{bmatrix} \Gamma_6 & -\Gamma_4 L & \Gamma_5 & \Gamma_3 L \\ -\Gamma_4 L & \Gamma_2 L^2 & -\Gamma_3 L & \Gamma_1 L^2 \\ \Gamma_5 & -\Gamma_3 L & (\Gamma_6 - \Omega^2 \bar{\alpha}) & \Gamma_4 L \\ \Gamma_3 L & \Gamma_1 L^2 & \Gamma_4 L & (\Gamma_2 - \Omega^2 \bar{\beta}) L^2 \end{bmatrix} \begin{Bmatrix} w_1 \\ w_2 \\ w_3 \\ w_4 \end{Bmatrix} = \begin{Bmatrix} 0 \\ 0 \\ f_3 \\ f_4 \end{Bmatrix} \quad (71)$$

272 Here f_3 and f_4 are amplitudes of the harmonic force and moment applied at the top of the
273 beam. We consider only a transverse force is applied to the top end, therefore, $f_3 = F_2$
274 and $f_4 = 0$. As $w_1 = w_2 = 0$ due to the fixed end, eliminating first two rows and columns,
275 and using the notation introduced in (27) we obtain

$$\frac{EI}{L^3} \begin{bmatrix} (\Gamma_6 - \Omega^2 \bar{\alpha}) & \Gamma_4 L \\ \Gamma_4 L & (\Gamma_2 - \Omega^2 \bar{\beta}) L^2 \end{bmatrix} \begin{Bmatrix} \delta^{(2)}(\omega) \\ \theta^{(2)}(\omega) \end{Bmatrix} = \begin{Bmatrix} F_2(\omega) \\ 0 \end{Bmatrix} \quad (72)$$

Solving this equation, we obtain the displacement and rotational response corresponding to the top point as

$$\delta^{(2)}(\omega) = \frac{(\Gamma_2 - \Omega^2 \bar{\beta})}{((\Gamma_6 - \Omega^2 \bar{\alpha})(\Gamma_2 - \Omega^2 \bar{\beta}) - \Gamma_4^2)} \frac{F_2(\omega) L^3}{EI} \quad (73)$$

$$\theta^{(2)}(\omega) = -\frac{\Gamma_4}{((\Gamma_6 - \Omega^2 \bar{\alpha})(\Gamma_2 - \Omega^2 \bar{\beta}) - \Gamma_4^2)} \frac{F_2(\omega) L^2}{EI} \quad (74)$$

276 *5.2. System with damped and flexible foundation*

277 For this case the general dynamic stiffness matrix in (67) need to be used. The
278 frequency dependent responses for the four degrees of freedom are obtained by solving
279 the 4×4 system of complex linear equations. The spatial response within the wind turbine
280 tower should be obtained with the complex shape functions as given in (18). We consider
281 two case of forcing. In the first case, only a transverse force acting on the top point is
282 considered. This is similar what discussed in the previous subsection. The forcing vector
283 is given by

$$\mathbf{f}(\omega) = \begin{Bmatrix} f_1(\omega) \\ f_2(\omega) \\ f_3(\omega) \\ f_4(\omega) \end{Bmatrix} = \begin{Bmatrix} 0 \\ 0 \\ F_2(\omega) \\ 0 \end{Bmatrix} \quad (75)$$

Solving the equilibrium equation (26) with the general dynamic stiffness matrix in (67), we obtain the displacement response corresponding to the bottom point as

$$\delta^{(1)}(\omega) = \left\{ \Omega^4 \bar{\alpha} \bar{\beta} \bar{\Gamma}_2 + (\bar{\beta} \Gamma_3^2 + (-\bar{\alpha} \Gamma_2 - \bar{\beta} \Gamma_6) \bar{\Gamma}_2 + \bar{\alpha} \Gamma_1^2) \Omega^2 - \Gamma_2 \Gamma_3^2 \right. \\ \left. - 2 \Gamma_1 \Gamma_3 \Gamma_4 + \bar{\Gamma}_2 (\Gamma_2 \Gamma_6 - \Gamma_4^2) - \Gamma_1^2 \Gamma_6 \right\} \frac{F_2(\omega) L^3}{EI \Delta_c} \quad (76)$$

In the above equation, Δ_c , the determinant of the general dynamic stiffness matrix in (67) is given by

$$\begin{aligned} \Delta_c = & \bar{\alpha}\bar{\beta}(\bar{\Gamma}_2\bar{\Gamma}_6 - \bar{\Gamma}_4^2)\Omega^4 + ((\bar{\alpha}\bar{\Gamma}_2 + \bar{\beta}\bar{\Gamma}_6)\Gamma_3^2 + 2\bar{\Gamma}_4(\bar{\alpha}\Gamma_1 - \bar{\beta}\Gamma_5)\Gamma_3 \\ & + (-\bar{\alpha}\bar{\Gamma}_6\Gamma_2 - b(-\Gamma_5^2 + \Gamma_6\bar{\Gamma}_6))\bar{\Gamma}_2 + \bar{\alpha}\bar{\Gamma}_6\Gamma_1^2 + \bar{\Gamma}_4^2(\bar{\alpha}\Gamma_2 + \bar{\beta}\Gamma_6))\Omega^2 + \Gamma_3^4 \\ & + (2\Gamma_1\Gamma_5 - \bar{\Gamma}_6\Gamma_2 - 2\bar{\Gamma}_4\Gamma_4 - \bar{\Gamma}_2\Gamma_6)\Gamma_3^2 + (2\Gamma_4\Gamma_5\bar{\Gamma}_2 + (-2\Gamma_4\bar{\Gamma}_6 - 2\Gamma_6\bar{\Gamma}_4)\Gamma_1 + 2\Gamma_2\Gamma_5\bar{\Gamma}_4)\Gamma_3 \\ & + ((-\Gamma_5^2 + \Gamma_6\bar{\Gamma}_6)\Gamma_2 - \Gamma_4^2\bar{\Gamma}_6)\bar{\Gamma}_2 + (\Gamma_5^2 - \Gamma_6\bar{\Gamma}_6)\Gamma_1^2 + 2\Gamma_1\Gamma_4\Gamma_5\bar{\Gamma}_4 - \bar{\Gamma}_4^2(\Gamma_2\Gamma_6 - \Gamma_4^2) \end{aligned} \quad (77)$$

The displacement corresponding to the top point is obtained as

$$\begin{aligned} \delta^{(2)}(\omega) = & \{\Gamma_3^2\bar{\Gamma}_2 + 2\Gamma_1\Gamma_3\bar{\Gamma}_4 + (-\Omega^2\bar{\beta} + \Gamma_2)\bar{\Gamma}_4 \\ & + \bar{\Gamma}_6(\Omega^2\bar{\beta}\bar{\Gamma}_2 + \Gamma_1^2 - \Gamma_2\bar{\Gamma}_2)\} \frac{F_2(\omega)L^3}{EI\Delta_c} \end{aligned} \quad (78)$$

284 Next we consider the case when only a transverse force acting on the bottom point.
285 The forcing vector is given by

$$\mathbf{f}(\omega) = \begin{Bmatrix} f_1(\omega) \\ f_2(\omega) \\ f_3(\omega) \\ f_4(\omega) \end{Bmatrix} = \begin{Bmatrix} F_1(\omega) \\ 0 \\ 0 \\ 0 \end{Bmatrix} \quad (79)$$

Solving the equilibrium equation, we obtain the displacement response corresponding to the bottom and top points as

$$\begin{aligned} \delta^{(1)}(\omega) = & \{\Omega^4\bar{\alpha}\bar{\beta}\bar{\Gamma}_2 + (\bar{\beta}\Gamma_3^2 + (-\bar{\alpha}\Gamma_2 - \bar{\beta}\Gamma_6)\bar{\Gamma}_2 + \bar{\alpha}\Gamma_1^2)\Omega^2 - \Gamma_2\Gamma_3^2 \\ & - 2\Gamma_1\Gamma_3\Gamma_4 + \bar{\Gamma}_2(\Gamma_2\Gamma_6 - \Gamma_4^2) - \Gamma_1^2\Gamma_6\} \frac{F_1(\omega)L^3}{EI\Delta_c} \end{aligned} \quad (80)$$

and

$$\begin{aligned} \delta^{(2)}(\omega) = & \{\Gamma_1\Gamma_3^2 + ((-\Omega^2\bar{\beta} + \Gamma_2)\bar{\Gamma}_4 + \bar{\Gamma}_2\Gamma_4)\Gamma_3 + \Gamma_1\Gamma_4\bar{\Gamma}_4 \\ & + \Gamma_5(\Omega^2\bar{\beta}\bar{\Gamma}_2 + \Gamma_1^2 - \Gamma_2\bar{\Gamma}_2)\} \frac{F_1(\omega)L^3}{EI\Delta_c} \end{aligned} \quad (81)$$

286 Although closed-form expressions have been obtained in the above expressions, a direct
287 numerical approach can also be employed if necessary.

288 The method developed here is essentially a frequency domain approach. The response
289 in the time-domain can be obtained using the usual Fourier transform of the frequency
290 domain data. It should be noted that geometric nonlinearity arising due to the compres-
291 sion of the wind turbine tower is already included in the formulation. However, material
292 nonlinearly is not considered in this initial work. Nonlinear behaviour in the stiffness
293 and damping properties can arise due to the interaction with the foundation (soil) and
294 aerodynamics of the turbine blades. From the point of view of this analysis, such non-
295 linearities will only impact the additional terms added to the dynamic stiffness matrix
296 in (31) and not the dynamic stiffness matrix itself. For weak material nonlinearities,
297 perturbation-based methods [35] can be developed for a more refined dynamic analysis.

298 **6. Numerical validation and illustration**

299 *6.1. Validation with respect to modal analysis*

300 Modal analysis [20] is the classical approach for dynamic response analysis of com-
 301 plex systems. When used in conjunction with the finite element method, the system is
 302 divided into a number of elements. Eigenvalues and eigenvectors are then calculated by
 303 solving the generalised eigenvalue problem involving the mass and stiffness matrices of the
 304 system. The dynamic response is calculated using the superposition of the eigenmodes.
 305 We consider a pinned-pinned beam to compare the results from the proposed dynamic
 306 stiffness approach with the modal analysis.

307 Dynamic response due to a harmonic moment at one end as shown in Fig. 3 is consid-
 ered. Using the notation introduced in (27) and considering the pinned-pinned boundary

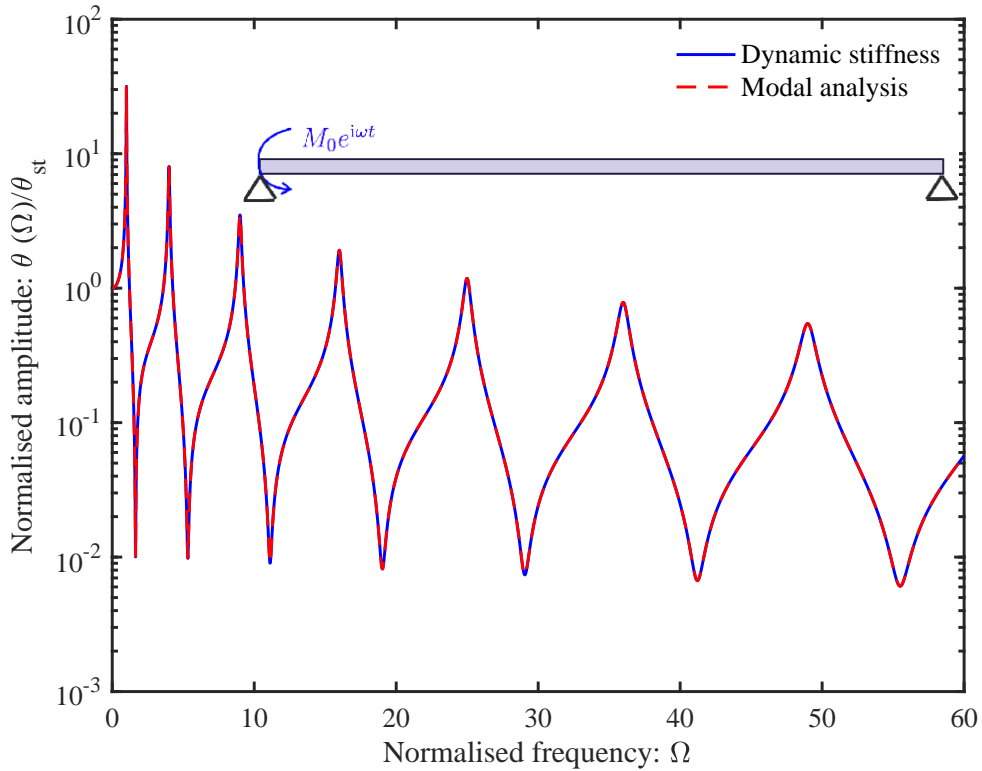


Fig. 3: The amplitude of the normalised rotation at the left end of a pinned-pinned beam due to an applied harmonic moment at the same point. The rotation is normalised with respect to the equivalent static response and plotted as a function of the normalised frequency. The damping factor values are $\xi_2 = 1 \times 10^{-2}$ and $\xi_1 = 0$.

308 condition, eliminating first and third rows and columns of the dynamic stiffness matrix
 309 in (31) we obtain

$$\frac{EI}{L^3} \begin{bmatrix} \Gamma_2 L^2 & \Gamma_1 L^2 \\ \Gamma_1 L^2 & \Gamma_2 L^2 \end{bmatrix} \begin{Bmatrix} \theta^{(1)}(\omega) \\ \theta^{(2)}(\omega) \end{Bmatrix} = \begin{Bmatrix} M_0(\omega) \\ 0 \end{Bmatrix} \quad (82)$$

311 Solving this equation, we derive the rotational responses and the two ends as

$$\begin{Bmatrix} \theta^{(1)}(\omega) \\ \theta^{(2)}(\omega) \end{Bmatrix} = \frac{L}{EI(\Gamma_2^2 - \Gamma_1^2)} \begin{Bmatrix} \Gamma_2 M_0 \\ -\Gamma_1 M_0 \end{Bmatrix} \quad (83)$$

312 For the special case when the moment is a static moment, considering $\omega \rightarrow 0$, from (47) we
313 have $\Gamma_2 \rightarrow 4$ and $\Gamma_2 \rightarrow 2$. Using this we obtain $\theta^{(1)} = M_0L/3EI$ and $\theta^{(2)} = -M_0L/6EI$.
314 They match exactly with the classical expressions. Hence the dynamic response given
315 by equation (83) is the generalisation of the static response to the damped case in the
316 frequency domain. The amplitude of the normalised rotation at the left end ($\theta^{(1)}$) is
317 shown Fig. 3. For the numerical calculations, $L = 1$ m, $EI/m = 10^4$ and $M_0 = 1$ are
318 used. In the same plot, the result obtained from the classical modal analysis is also shown.
319 The dynamic stiffness method and the modal analysis match exactly. While the dynamic
320 stiffness approach uses only one element, 100 elements were used for the modal analysis.
321 This requires the solution of a general eigenvalue problem with 200×200 dimensional
322 matrices. This comparative analysis clearly demonstrates not only the computational
323 efficiency of the dynamic stiffness method but also the fact that the complete damped
324 dynamic response can be obtained using simple closed-form expressions as in equation
325 (83). Next, we apply the proposed approach to a practical wind turbine problem.

326 6.2. Illustrative example

327 The analytical formulations derived in the previous sections are presented in terms of
328 non-dimensional parameters. This provides a convenient and general approach to consider
329 dynamic response analysis of wide range of wind turbine structures in a unified manner.
330 In this section we provide numerical illustrations to demonstrate this process.

331 Example of a wind turbine used in reference [16] is employed. The numerical values
of the main parameters are summarised in Table 2. The moment of inertia of the circular

Turbine Structure Properties	Numerical values
Length (L)	81 m
Average diameter (D)	3.5m
Thickness (t_h)	0.075 mm
Mass density (ρ)	7800 kg/m ³
Young's modulus (E)	2.1×10^{11} Pa
Mass density (ρ_t)	7800 kg/m ³
Rotational speed (ϖ)	22 r.p.m = 0.37 Hz
Top mass (M)	130,000 kg
Rated power	3 MW

Table 2: Material and geometric properties of the turbine structure considered for dynamic response analysis.

332
333 cross section can be obtained as

$$I = \frac{\pi}{64}D^4 - \frac{\pi}{64}(D - t_h)^4 \approx \frac{1}{16}\pi D^3 t_h = 0.6314m^4 \quad (84)$$

334 The mass density per unit length of the system can be obtained as

$$m = \rho A \approx \rho \pi D t_h / 2 = 3.1817 \times 10^3 \text{ kg/m} \quad (85)$$

335 Using these, the mass ratio $\alpha = 00.5044$ and the nondimensional axial force $\nu = 0.0652$.
336 The rotary inertia parameter β is assumed to be zero. We also obtain the natural frequency

337 scaling parameter as

$$c_0 = \frac{EI}{mL^4} = 0.9682 \text{ s}^{-1} \quad (86)$$

338 The radius of gyration of the wind turbine is given by

$$r = \sqrt{\frac{I}{A}} = \frac{1}{4} \sqrt{D^2 + (D - t_h)^2} \approx \frac{D}{2\sqrt{2}} = 1.2374m \quad (87)$$

339 Therefore, the nondimensional radius of gyration $\mu = r/L = 0.0151$. From Eq. (7) we
340 therefore have

$$\tilde{\nu} = \nu + 2.2844 \times 10^{-4} \Omega^2 \approx \nu \quad (88)$$

341 The non-dimensional parameters corresponding to the foundation stiffness are given by
342 $\eta_l = 3000, \eta_r = 30, \eta_{rl} = -60$. Details of the natural frequency analysis analysis can be
343 found in reference [16].

344 Here we focus on the dynamic response calculations. For this, the key additional
345 parameters necessary are the seven damping parameters introduced in the paper. We
346 consider three cases of damping parameters. In the first case, only the tower is damped.
347 In the second case, we consider only the aerodynamic damping at the nacelle of the wind
348 turbine. The last case is when damping is present only at the foundation. These cases are
349 considered to understand and differentiate the impact of different damping parameters.
350 In Fig. 4 we show the amplitude of the normalised lateral deflection at the bottom and top
351 end of the wind turbine due to an applied harmonic force at the top end. The response
352 at the bottom point is significantly smaller compared to the response at the top point as
353 expected. The peaks in the response correspond to the natural frequencies of the system.
354 There are three natural frequencies within the frequency range considered. In the same
355 plot, the response at the top end when the foundation is fixed (like a cantilever) is also
356 shown. This system is stiffer as it shows higher natural frequencies compared to wind
357 turbine with a flexible foundation. The difference between the two case increase in hinger
358 frequencies (marked in Fig. 4).

359 The amplitude of the normalised lateral deflections are shown in Fig. 5 when only
360 the aerodynamic damping at the nacelle of the wind turbine is considered. This case
361 demonstrates a considerable damped response to the wind turbine. The response at top
362 point (where the dampers are) diminishes sharply at higher frequencies to an extent that
363 it almost matches with that at the bottom point (marked in Fig. 5).

364 In Fig. 6, the amplitude of the normalised lateral deflections are shown when damping
365 is present only at the foundation. We can see orders of magnitude difference in response
366 between the case of the fixed and the flexible foundation case (marked in Fig. 6). This is
367 arising because the tower with the fixed foundation is effectively undamped and therefore
368 has a very high response around the resonance frequencies. This plot also demonstrates
369 that the dynamic response of the wind turbine can be controlled with properly designed
370 dampers at the foundation.

371 Explicit consideration of physics-based damping factors is a key novel feature of the
372 proposed approach. All the seven crucial damping factors identified here are summarised
373 in Table 3. Some suggested values of the damping factors are given in the table. To un-
374 derstand the effects of different damping factors we consider two extreme cases comprising
375 of lower and higher values given in the table. In Fig. 7 The amplitude of the normalised

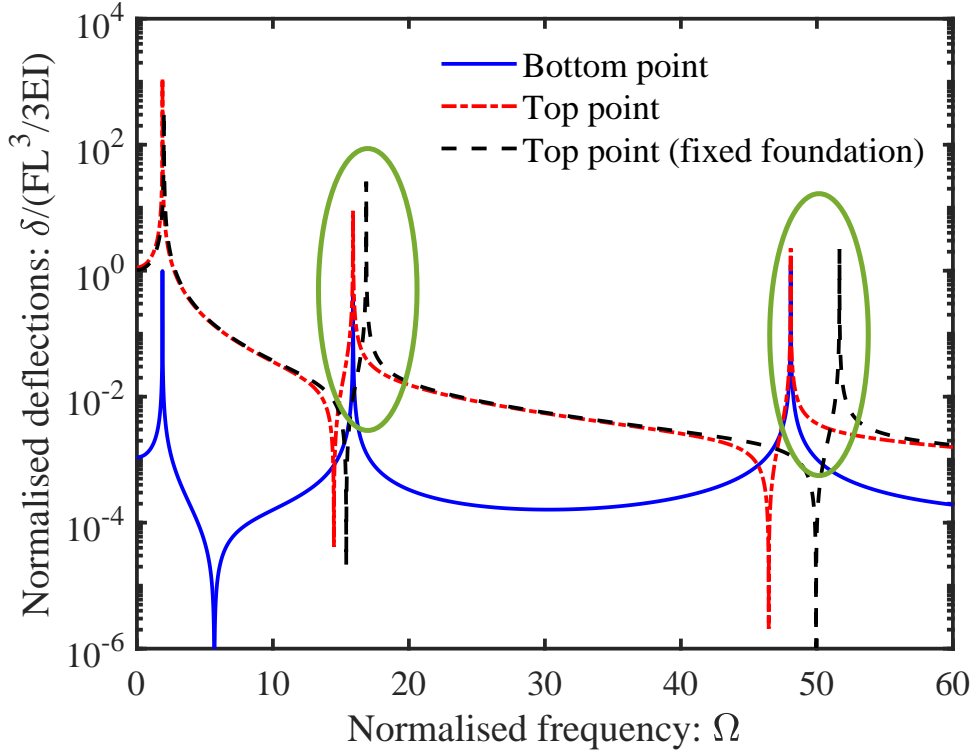


Fig. 4: The amplitude of the normalised lateral deflection at the bottom and top end of the wind turbine due to an applied harmonic force at the top end plotted as functions of the normalised frequency. The displacement is normalised with respect to the equivalent static response. The damping factor values are $\xi_2 = 1 \times 10^{-3}$ and all the others are zero.

376 lateral deflection at the top end of the wind turbine due to an applied harmonic force at
 377 the top end is shown for low and high values of the damping factors given in Table 3. It
 378 can be observed that a significant difference in the dynamic response, particular in the
 379 first mode, can occur due to the difference in the damping factors values. The method
 380 developed in this paper can comprehensively incorporate different physics-based damping
 381 factors in a unified manner. This presents a platform for analysing and understanding
 382 the impact of damping factors on the dynamic design of wind turbines.

383 7. Conclusion

384 The quantification of the dynamic response of wind turbine towers due to various
 385 external forces is of paramount importance. A physics-based analytical approach leading
 386 to closed-form expressions of essential dynamic response quantities was presented. The
 387 route to this analytical derivation has three key steps. Firstly, noting that the wind
 388 turbine tower is a beam-like structure, the dynamic stiffness matrix of a beam with axial
 389 compressive force is derived exactly. This is achieved using transcendental displacement
 390 functions which are exact solutions of the governing partial differential equation with
 391 appropriate boundary conditions. Due to the presence of damping, the elements of the
 392 dynamic stiffness coefficients are complex-valued functions of the frequency. Secondly, to

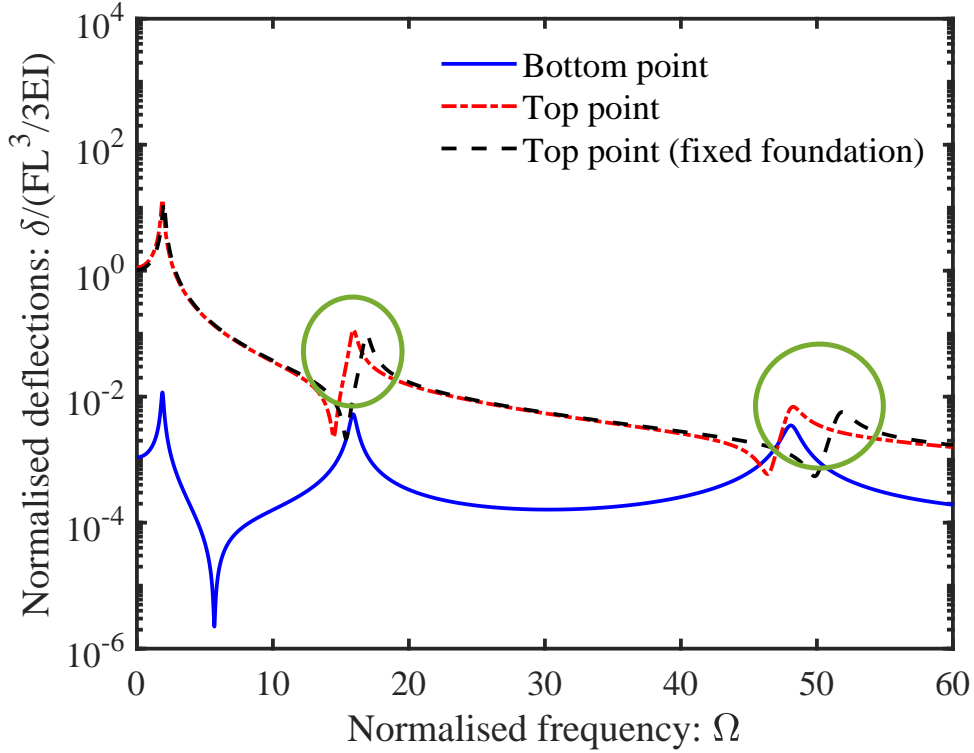


Fig. 5: The amplitude of the normalised lateral deflection at the bottom and top end of the wind turbine due to the applied harmonic excitation at the top end plotted as functions of the normalised frequency. The displacement is normalised with respect to the equivalent static response. The damping factor values are $\xi_M = 1 \times 10^{-1}$, $\xi_J = 1 \times 10^{-2}$ and all the others are zero.

393 take account of the foundation stiffness and damping, the mass and rotary inertia of the
 394 nacelle along with aerodynamic damping, additional elements are added to the pristine
 395 dynamic stiffness matrix derived in the first step. Finally, resulting compound dynamic
 396 stiffness is inverted with appropriate boundary conditions to obtain the dynamic response
 397 through closed-form expressions. These expressions are exact and valid for any frequency
 398 of the applied forcing. Direct comparison with modal analysis confirms that the proposed
 399 dynamic stiffness approach produces the same results. However, unlike the classical modal
 400 analysis, the determination of natural frequencies and mode shapes are not necessary and
 401 only one element is sufficient to obtain the dynamic response across the frequency ranges.

402 The analytical results derived in the paper are in terms of several non-dimensional
 403 parameters. This makes them general and applicable to any wind turbine structures. As
 404 the method is essentially a frequency domain approach, it is straightforward to obtain the
 405 output spectral function from any given input spectral function of the applied forcing.
 406 A key novel feature is the introduction of seven physically-based damping factors. They
 407 have been classed into three distinct groups, (a) velocity and strain-dependent damping
 408 factors of the wind turbine tower, (b) mass and rotary damping factors of the nacelle,
 409 and (c) lateral, rotational and cross damping factors of the foundation. This approach
 410 enables a more precise route to the damping quantification which is important not only
 411 for the response-amplitude determination but also for long-term fatigue prediction. It is

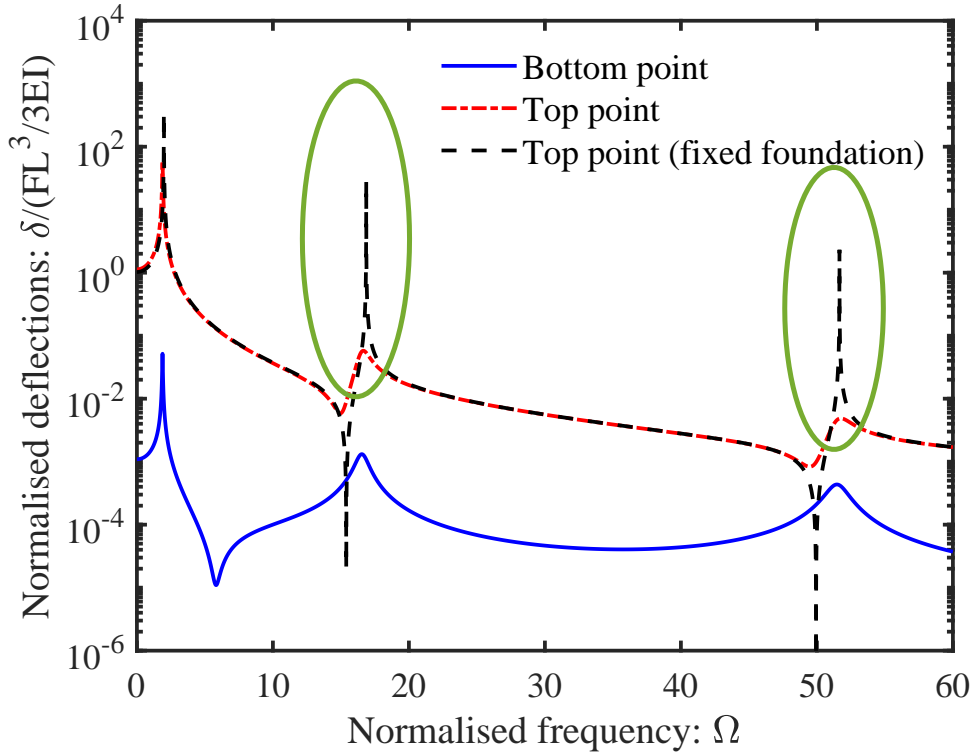


Fig. 6: The amplitude of the normalised lateral deflection at the bottom and top end of the wind turbine due to the applied harmonic excitation at the top end plotted as functions of the normalised frequency. The displacement is normalised with respect to the equivalent static response. The damping factor values are $\xi_l = 1 \times 10^{-1}$, $\xi_r = 1 \times 10^{-1}$, $\xi_{lr} = 1 \times 10^{-1}$ and all the others are zero.

412 not possible to incorporate damping in this physical manner using the conventional modal
 413 approach. Limited numerical results shown in the paper clearly demonstrate in the impact
 414 of different damping groups on the dynamic response due to harmonic excitation. The
 415 numerical analysis also shows how the dynamic response in the higher modes can be
 416 obtained simply using the formulae given in the paper. Future research is needed towards
 417 the experimental determination of the seven new damping factors introduced here.

418 References

- 419 [1] L. Arany, S. Bhattacharya, Simplified load estimation and sizing of suction anchors for spar buoy
 420 type floating offshore wind turbines, *Ocean Engineering* 159 (2018) 348–357.
 421 [2] R. De Risi, S. Bhattacharya, K. Goda, Seismic performance assessment of monopile-supported off-
 422 shore wind turbines using unscaled natural earthquake records, *Soil Dynamics and Earthquake*
 423 *Engineering* 109 (2018) 154–172.
 424 [3] S. Bhattacharya, *Design of foundations for offshore wind turbines*, Wiley Online Library.
 425 [4] O. Adedipe, F. Brennan, A. Kolios, Corrosion fatigue load frequency sensitivity analysis, *Marine*
 426 *Structures* 42 (2015) 115–136.
 427 [5] G. Chortis, A. Askarnejad, L. Prendergast, Q. Li, K. Gavin, Influence of scour depth and type on
 428 p–y curves for monopiles in sand under monotonic lateral loading in a geotechnical centrifuge, *Ocean*
 429 *Engineering* (2020) 106838.
 430 [6] H. Zuo, K. Bi, H. Hao, Using multiple tuned mass dampers to control offshore wind turbine vibrations
 431 under multiple hazards, *Engineering Structures* 141 (2017) 303–315.

Damping category	Damping factor	Notation	Analytical formula	Suggested values
A: Wind turbine tower damping	Strain-rate-dependent damping factor	ξ_1	$\frac{c_1}{L^2\sqrt{mEI}}$	$10^{-3} - 10^{-5}$
	Velocity-dependent damping factor	ξ_2	$\frac{c_2L^2}{\sqrt{mEI}}$	$10^{-2} - 10^{-3}$
B: Foundation/soil damping	Lateral foundation damping factor	ξ_l	$\frac{c_lL}{\eta_l\sqrt{mEI}}$	$10^{-1} - 10^{-2}$
	Rotational foundation damping factor	ξ_r	$\frac{c_r}{\eta_rL\sqrt{mEI}}$	$10^{-2} - 10^{-3}$
	Cross foundation damping factor	ξ_{lr}	$\frac{c_{lr}}{\eta_{rl}\sqrt{mEI}}$	$10^{-1} - 10^{-4}$
C: Damping corresponding to the nacelle	Aerodynamic mass damping factor	ξ_M	$\frac{c_ML}{\sqrt{mEI}}$	$10^{-1} - 10^{-3}$
	Aerodynamic rotary damping factor	ξ_J	$\frac{c_J}{L\sqrt{mEI}}$	$10^{-2} - 10^{-4}$

Table 3: Physics-based damping factors necessary for the dynamic analysis of wind turbines.

- 432 [7] T. Sellami, H. Berriri, A. M. Darcherif, S. Jelassi, M. F. Mimouni, Modal and harmonic analysis of
433 three-dimensional wind turbine models, *Wind Engineering* 40 (6) (2016) 518–527.
- 434 [8] A. Banerjee, T. Chakraborty, V. Matsagar, Stochastic dynamic analysis of an offshore wind tur-
435 bine considering frequency-dependent soil–structure interaction parameters, *International Journal*
436 *of Structural Stability and Dynamics* 18 (06) (2018) 1850086.
- 437 [9] P. D. Scavounos, Y. Zhang, Y. Ma, D. F. Larson, Offshore wind turbine nonlinear wave loads and
438 their statistics, *Journal of Offshore Mechanics and Arctic Engineering* 141 (3).
- 439 [10] Q. Wang, Z. Wang, B. Fan, Coupled bending and torsional vibration characteristics analysis of
440 inhomogeneous wind turbine tower with variable cross section under elastic constraint, *Applied*
441 *Mathematical Modelling*.
- 442 [11] C. V. C. Júnior, R. C. de Alencar Araújo, C. M. C. de Souza, A. C. A. Ferreira, P. M. V. Ribeiro, A
443 collocation method for bending, torsional and axial vibrations of offshore wind turbines on monopile
444 foundations, *Ocean Engineering* 217 (2020) 107735.
- 445 [12] R. He, A. M. Kaynia, J. Zhang, W. Chen, Seismic response of monopiles to vertical excitation in
446 offshore engineering, *Ocean Engineering* 216 (2020) 108120.
- 447 [13] S. K. Patra, S. Haldar, Fore-aft and the side-to-side response of monopile supported offshore wind
448 turbine in liquefiable soil, *Marine Georesources & Geotechnology* (2020) 1–22.
- 449 [14] M. Zhao, Z. Gao, P. Wang, X. Du, Response spectrum method for seismic analysis of monopile
450 offshore wind turbine, *Soil Dynamics and Earthquake Engineering* 136 (2020) 106212.
- 451 [15] W. Jiang, C. Lin, M. Sun, Seismic responses of monopile-supported offshore wind turbines in soft
452 clays under scoured conditions, *Soil Dynamics and Earthquake Engineering* 142 (2021) 106549.
- 453 [16] S. Adhikari, S. Bhattacharya, Dynamic analysis of wind turbine towers on flexible foundations, *Shock*

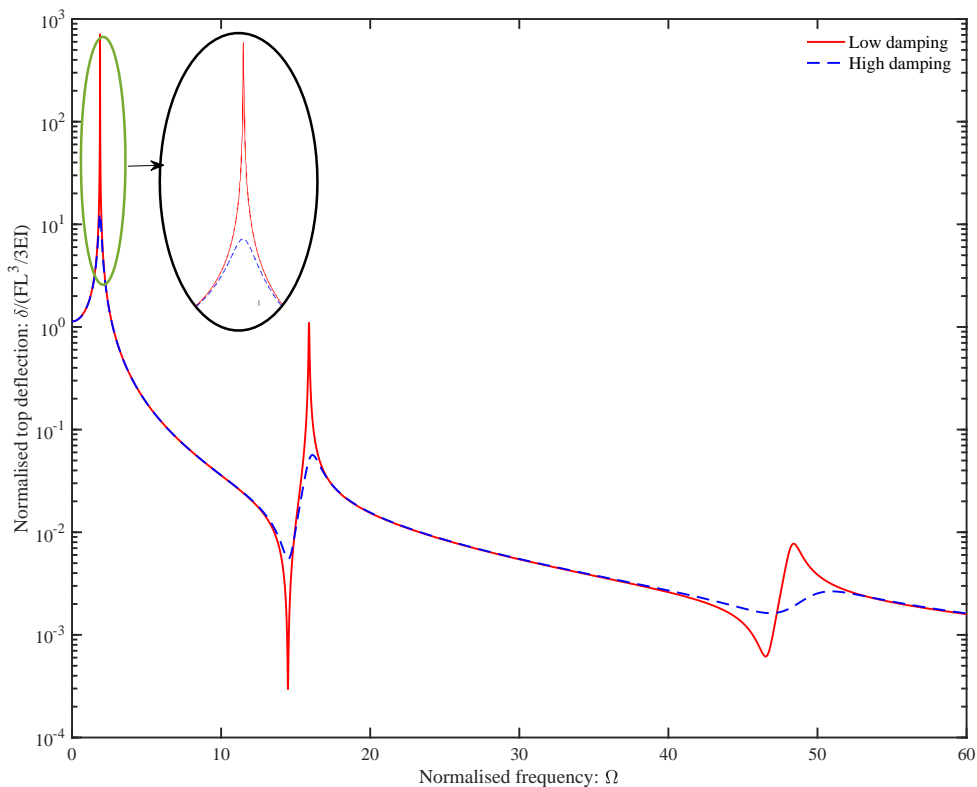


Fig. 7: The amplitude of the normalised lateral deflection at the top end of the wind turbine due to an applied harmonic force at the top end plotted as a function of the normalised frequency. The two cases shown correspond to low and high values of the damping factors given in Table 3.

- 454 and *Vibration* 19 (1) (2012) 37–56.
- 455 [17] S. Adhikari, S. Bhattacharya, *Vibrations of wind-turbines considering soil-structure interaction*,
456 *Wind and Structures, An International Journal* 14 (2) (2011) 85–112.
- 457 [18] S. Bhattacharya, S. Adhikari, *Experimental validation of soil-structure interaction of offshore wind*
458 *turbines*, *Soil Dynamics and Earthquake Engineering* 31 (4-6) (2011) 805–816.
- 459 [19] L. Arany, S. Bhattacharya, S. Adhikari, S. J. Hogan, J. Macdonald, *An analytical model to pre-*
460 *dict the natural frequency of offshore wind turbines on three-spring flexible foundations using two*
461 *different beam models*, *Soil Dynamics and Earthquake Engineering* 74 (1) (2015) 40–45.
- 462 [20] L. Meirovitch, *Principles and Techniques of Vibrations*, Prentice-Hall International, Inc., New Jersey,
463 1997.
- 464 [21] M. Paz, *Structural Dynamics: Theory and Computation*, 2nd Edition, Van Nostrand, Reinhold,
465 1980.
- 466 [22] A. Y. T. Leung, *Dynamic Stiffness and Substructures*, Springer-Verlag, London, UK, 1993.
- 467 [23] C. S. Manohar, S. Adhikari, *Dynamic stiffness of randomly parametered beams*, *Probabilistic Engi-*
468 *neering Mechanics* 13 (1) (1998) 39–51.
- 469 [24] J. R. Banerjee, *Dynamic stiffness formulation for structural elements: A general approach*, *Computer*
470 *and Structures* 63 (1) (1997) 101–103.
- 471 [25] S. Adhikari, C. S. Manohar, *Transient dynamics of stochastically parametered beams*, *ASCE Journal*
472 *of Engineering Mechanics* 126 (11) (2000) 1131–1140.
- 473 [26] J. F. Doyle, *Wave Propagation in Structures*, Springer Verlag, New York, 1989.
- 474 [27] S. Adhikari, T. Murmu, M. McCarthy, *Dynamic finite element analysis of axially vibrating nonlocal*
475 *rods*, *Finite Elements in Analysis and Design* 63 (1) (2013) 42–50.
- 476 [28] X. Liu, J. Banerjee, *A spectral dynamic stiffness method for free vibration analysis of plane elasto-*

- 477 dynamic problems, *Mechanical Systems and Signal Processing* 87 (2017) 136–160.
- 478 [29] S. Adhikari, D. Karlicic, X. Liu, Dynamic stiffness method for nonlocal damped nano-beams on
479 elastic foundation, *European Journal of Mechanics-A/Solids* 86 (3-4) (2021) 104144.
- 480 [30] D. J. Inman, *Engineering Vibration*, Prentice Hall PTR, NJ, USA, 2003.
- 481 [31] M. Géradin, D. Rixen, *Mechanical Vibrations*, 2nd Edition, John Wiley & Sons, New York, NY,
482 1997, translation of: *Théorie des Vibrations*.
- 483 [32] M. Petyt, *Introduction to Finite Element Vibration Analysis*, Cambridge University Press, Cam-
484 bridge, UK, 1998.
- 485 [33] D. Dawe, *Matrix and Finite Element Displacement Analysis of Structures*, Oxford University Press,
486 Oxford, UK, 1984.
- 487 [34] S. Bisoi, S. Haldar, Dynamic analysis of offshore wind turbine in clay considering soil–monopile–
488 tower interaction, *Soil Dynamics and Earthquake Engineering* 63 (2014) 19–35.
- 489 [35] A. H. Nayfeh, D. T. Mook, *Nonlinear oscillations*, John Wiley & Sons, New York, NY, 1979.